Geometric heat pump and no-go restrictions of nonreciprocity in modulated thermal diffusion

Zi Wang ⬤,[*] Jiangzhi Chen,[*] and Jie Ren ⬤[†]

Center for Phononics and Thermal Energy Science, China-EU Joint Lab on Nanophononics,
Shanghai Key Laboratory of Special Artificial Microstructure Materials and Technology,
School of Physics Science and Engineering, Tongji University, Shanghai 200092, China

Thermodynamics strongly restricts the direction of heat flow in static macroscopic thermal diffusive systems. To overcome this constraint, spatiotemporal modulated systems are used instead. Here, we unveil the underlying geometric heat pump effect in macroscopic driven thermal diffusion, which is crucial for achieving thermal nonreciprocity. We obtain a geometric expression to formulate the nontrivial current in a driven system, manifesting as an extra pumped heat ably diffusing from cold to hot that has no analogy in static setups. Moreover, we analyze the underlying geometric curvature of driven diffusive systems and derive no-pumping restriction theorems that constrain the thermal action under modulations and guide the optimization of driving protocols. Following the restrictions from geometry, we finally implement a minimum experiment and observe the predicted pumped heat in the absence of thermal bias at every instant, which is independent of the driving speed in the adiabatic limit, clearly validating the geometric theory. An extension of the geometric pump effect and no-pumping restrictions to macroscopic mass diffusion governed by Fick's law is also discussed. These results pave the way for designing and implementing nonreciprocal and topological diffusive systems under spatiotemporal modulations.

Introduction. Recently, there has been a surge of interest in thermal transport [1–4], which is also fundamentally central in nonequilibrium statistical physics [5–7]. Versatile thermal devices [8–11] and heat manipulations have been realized by delicately designing the spatial parameter distribution [12–16], where heat always flows from hot to cold as restricted by thermodynamics. To construct thermal nonreciprocity and cold-to-hot heat pumps to break the constraint, temporal drivings are applied to quantum systems [17–20] and thermal systems, producing novel effects, such as ratcheting heat flow [21,22], driven heat engines [23], nonreciprocal thermal metamaterials [24], dynamic refrigeration [25], radiative heat shuttling [26], adiabatic thermal radiation pumps [27], as well as intriguing experimental observations, such as superior electrocaloric cooling [28], and non-Hermitian thermal [29] and topological thermal [30] dynamics.

Considering the versatility caused by driving, it is challenging to grasp the underlying universal mechanisms. The geometry emerges as one of the most insightful ideas. A geometric phase was originally proposed in closed quantum systems [31,32], and later generalized to the scattering process in open quantum systems [33] and also to the full counting statistics [34] in stochastic pumps [35–37], which is manifested as an additional term obtained after a periodic modulation. Concerning the heat transport process, a similar geometric effect was unveiled in an anharmonic quantum

junction [38], which induced an additional pumped heat from cold to hot during periodic driving, a so-called geometric heat pump. Subsequently, the geometric heat pump effect caused a plethora of research on its manifestation in nanosized open quantum [39–41] and classical coupled oscillators [42]. Also, recently, connections of the geometric effect with entropy production [43], heat engines [44–46], and nonadiabatic controls [47,48] have been established. These works emphasize the fertile status of the geometric heat pump effect [49].

Despite massive theoretical attention and broad implications, the theory of the geometric heat pump effect has been confined so far to quantum nanoscale and microscopic stochastic systems, and has not yet been observed experimentally. Therefore, in view of the extensive interest in nonreciprocal spatiotemporal thermal devices at the macroscopic scale, fundamental questions naturally arise: Is the geometric heat pump effect universally present in macroscopic driven thermal diffusion? What is the general theory of geometric pumping and no-go restrictions on thermal nonreciprocity? How can we observe the effect macroscopically?

Here, we resolve the above questions. We excavate the geometric heat contribution in addition to the conventional dynamic heat flow in general driven diffusive systems, illustrated in Fig. 1. This geometric theory establishes a universal framework for studying the driven diffusion. It automatically yields no-pumping theorems that constrain the thermal nonreciprocity under spatiotemporal modulations. We further elaborate a minimal experimental setup to successfully demonstrate our theory. Our work may further advance the field of nonreciprocal thermal transport, geometric heat engines, and topological thermal devices. The extension of the geometric pump effect

---

[*]These authors contributed equally to this work.
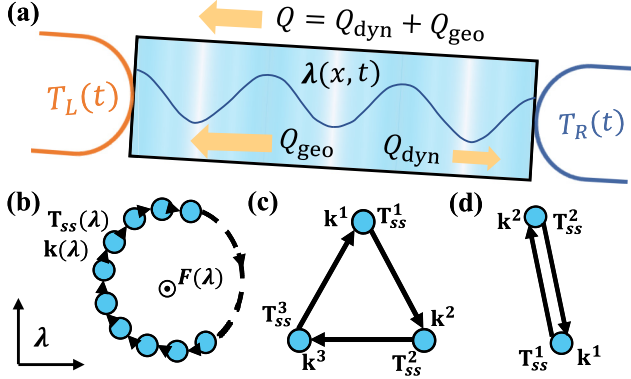[†]Corresponding author: xonics@tongji.edu.cn

FIG. 1. A diagram of driven diffusive systems from continuous protocols to Trotterized discrete protocols. (a) The anomalous heat transport as a competition between cold-to-hot geometric heat Q_{geo} and hot-to-cold dynamic heat Q_{dyn}. (b) The continuous driving path. Solid dots denote states in the parameter space $\boldsymbol{\lambda}$ (reservoir temperature, thermal conductance, etc.). Q_{geo} is induced by the intrinsic geometric curvature $\mathbf{F}(\boldsymbol{\lambda})$. $\mathbf{T}_{ss}$ denotes the instantaneous steady state temperature and vector $\mathbf{k}$ is determined by the diffusion dynamics dual to the space of $\mathbf{T}_{ss}$. (c) A Trotterized discrete state protocol forming a triangle cycle. (d) The minimum two-state switching protocol.
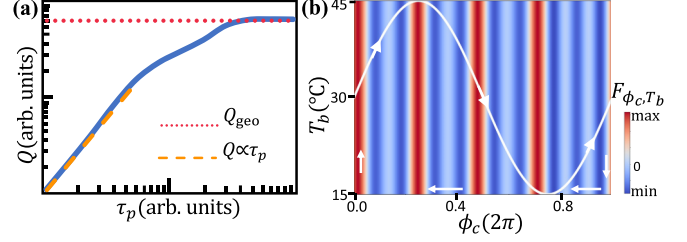

FIG. 2. The geometric heat pump effect and the origin of its geometric curvature in a driven one-dimensional diffusive chain. (a) The heat pumped by the driving reservoir $\mathbf{T}_b$ and the conductance $\mathcal{K}_c$ and $\mathcal{K}_b$. τ_p is the driving period. (b) The origin of Q_{geo} as a nontrivial curvature F_{ϕ_c,T_b}. The sinusoidal line represents the protocol. The integration of F encircled by the arrowed contour is Q_{geo}. The protocol of the reservoir temperature is $\mathbf{T}_b(t) = T_0[\sin(2\pi t)/2 + 1](1,1)^T$ and that of conductance at the edge n ($n = 0, 1, \ldots, n_v$) is $\kappa_n = \frac{\kappa}{2}[\sin(\phi_n + \phi_c) + 1]$. $\phi_n \equiv 2\pi n_p n/(n_v + 1)$ designates different edges with out-of-phase conductance. $\phi_c \equiv 2\pi t/\tau_p$ ($0 \leqslant t < \tau_p$) parametrizes the conductance protocol. n_p is the number of space periods and n_v is the number of vertices in the chain. In this figure, we select $T_0 = 30\,°C$, $n_v = 12$, $n_p = 3$, $\kappa = 1.20$ W/K, and the vertex heat capacity is uniform $C_n = 0.833$ J/K ($n = 1, \ldots, n_v$).

and no-pumping restrictions to general Fick's diffusions is straightforward.

Geometric heat pump effect. We begin by recapitulating the well-known classical thermal diffusion, governed by the Fourier's law [50] $\mathbf{J} = -\kappa \nabla T(x,t)$ and the continuity equation $\partial_t E = -\nabla \cdot \mathbf{J}$, where E is the internal energy density and κ is the conductivity. We consider the diffusion on a conduction network. Describing the central system temperature using vector $\mathbf{T}_c$ and taking into account the boundary reservoirs $\mathbf{T}_b$, the heat flow during the linear conduction is given by $\mathbf{J} = \mathcal{K}_c\mathbf{T}_c + \mathcal{K}_b\mathbf{T}_b$, where the conduction matrix $\mathcal{K}_c$ ($\mathcal{K}_b$) depicts the heat conduction induced within the system itself (by coupling to thermal reservoirs). The heat flow $\mathbf{J}$ is a column vector containing current distributions. Considering the continuity equation, we have $\partial_t\mathbf{T}_c = \mathcal{L}\mathbf{J}$ [24]. Here, $\mathcal{L} \equiv \mathcal{C}^{-1}\mathcal{D}$. The diagonal matrix $\mathcal{C}$ contains the heat capacity and $\mathcal{D}$ is the negative divergence matrix (the discrete version of $-\nabla\cdot$).

The evolution of the system's temperature distribution follows

$$\frac{\partial}{\partial t}\mathbf{T}_c = \mathcal{M}_c\mathbf{T}_c + \mathcal{M}_b\mathbf{T}_b, \tag{1}$$

where $\mathcal{M}_c \equiv \mathcal{L}\mathcal{K}_c$ and $\mathcal{M}_b \equiv \mathcal{L}\mathcal{K}_b$. The invertible Laplacian matrix $\mathcal{M}_c$ depicts the heat diffusion within the central system itself and the noninvertible $\mathcal{M}_b$ depicts the heat diffusion from boundary reservoirs to the central system. The notation is exemplified in Sec. I of the Supplemental Material [51].

As shown in Fig. 1(a), the system is generally modulated by nonadiabatic and cyclic protocols $\boldsymbol{\lambda}(t + \tau_p) = \boldsymbol{\lambda}(t)$, where τ_p is the temporal period. We rewrite Eq. (1) as $\mathbf{T}_c = \mathbf{T}_{ss} + \mathcal{M}_c^{-1}\partial_t\mathbf{T}_c$, with $\mathbf{T}_{ss} \equiv -\mathcal{M}_c^{-1}\mathcal{M}_b\mathbf{T}_b$ being the instantaneous steady state temperature. One can see that the accumulated current $Q \equiv \int_0^{\tau_p} dt\mathbf{1} \cdot \mathbf{J}(t)$ during one driving period τ_p is

naturally composed of two contributions, termed the dynamic and geometric components, respectively:

$$Q_{dyn} := \int_0^{\tau_p} dt\mathbf{1} \cdot (\mathcal{K}_c\mathbf{T}_{ss} + \mathcal{K}_b\mathbf{T}_b), \tag{2}$$

$$Q_{geo} := \int_0^{\tau_p} dt\mathbf{1} \cdot \mathcal{K}_c\mathcal{M}_c^{-1} \cdot \partial_t\mathbf{T}_c. \tag{3}$$

Here, $\mathbf{1}$ is a constant vector projecting $\mathbf{J}$ onto the interested current component. For example, we may choose $\mathbf{1}_j = \delta_{ij}$, with δ_{ij} being the Kronecker delta, to study the current component i. The other normalized $\mathbf{1}$ is useful for studying even a linear combination of several currents. These two contributions to $Q = Q_{geo} + Q_{dyn}$ are distinguished by their different natures. Q_{dyn} is simply an average of instantaneous steady current, while the nontrivial Q_{geo} has no analogy in static systems, rendering more flexible modulated diffusion. It is worthy noting that Q_{geo} is reminiscent of the nonadiabatic Aharonov-Anandan phase in a general cyclic driven Hamiltonian [52].

In the fast driving regime around the infinite-frequency limit, $\mathbf{T}_c(t)$ is nearly frozen, due to the separation of the timescale between the driving and the system's response [53]. The geometric Q_{geo} vanishes and $Q_{dyn} \propto \tau_p$ remains, as shown by the dashed line in Fig. 2(a). We prove that in the infinite-frequency limit, Q is determined by the renormalized stroboscopic state, so that the average heat flow $\langle J \rangle \equiv Q/\tau_p$ is independent on τ_p. Specifically, we find that $\langle J \rangle = \mathbf{1} \cdot (\langle\mathcal{K}_c\rangle \mathbf{T}_{st} + \langle\mathcal{K}_b\mathbf{T}_b\rangle)$, where $\mathbf{T}_{st} \equiv -\mathcal{M}_{eff}^{-1}\langle\mathcal{M}_b\mathbf{T}_b\rangle$ is the stroboscopic system temperature, with the effective operator being $\mathcal{M}_{eff} \equiv \langle\mathcal{M}_c\rangle$. Here, $\langle O \rangle \equiv (1/\tau_p)\int_0^{\tau_p} dtO(t)$ is a time average of an arbitrary temporal periodic quantity O.

In slow driving regime, $\mathbf{T}_c$ approaches the instantaneous steady states $\mathbf{T}_{ss}$, according to the adiabatic perturbation

theory [54]. The geometric heat component

$$Q_{\text{geo}} = \int_0^{\tau_p} dt\, \mathbf{k} \cdot \frac{\partial \mathbf{T}_{\text{ss}}}{\partial \lambda_\mu} \dot{\lambda}_\mu = \oint_{\partial\Omega} d\boldsymbol{\lambda} \cdot \mathbf{A} \tag{4}$$

is now independent of τ_p and completely determined by the geometric connection $A_\mu = \mathbf{k} \cdot \nabla_{\lambda_\mu} \mathbf{T}_{\text{ss}}$ with the driven parameters $\boldsymbol{\lambda}(t) = \{\lambda_\mu(t)\}$ ($0 \leqslant t < \tau_p$) forming the closed path $\partial\Omega$. $\mathbf{k} \equiv \mathbf{1} \cdot \mathcal{K}_c \mathcal{M}_c^{-1}$ is the row vector mapping the variation of $\mathbf{T}_{\text{ss}}$ into the interested heat current and is in the dual space of $\mathbf{T}_{\text{ss}}$. A_μ here is reminiscent of the original Berry connection [31] and the counterpart in microscopic stochastic systems [38,42]. With the aid of the Stokes formula, Q_{geo} can also be formulated as

$$Q_{\text{geo}} = \int_\Omega F_{\mu\nu}(\boldsymbol{\lambda}) dS_{\mu\nu},$$

$$F_{\mu\nu}(\boldsymbol{\lambda}) := \frac{\partial \mathbf{k}}{\partial \lambda_\mu} \cdot \frac{\partial \mathbf{T}_{\text{ss}}}{\partial \lambda_\nu} - \frac{\partial \mathbf{k}}{\partial \lambda_\nu} \cdot \frac{\partial \mathbf{T}_{\text{ss}}}{\partial \lambda_\mu}. \tag{5}$$

The antisymmetric tensor $F_{\mu\nu}(\boldsymbol{\lambda}) = -F_{\nu\mu}(\boldsymbol{\lambda})$ clearly has the meaning of geometric curvature [shown in Fig. 1(b)] and the area Ω is encircled by $\partial\Omega$. $dS_{\mu\nu}$ is the surface element. For a detailed derivation, see Sec. II of the Supplemental Material [51].

Considering a protocol parametrized by the phase ϕ_c of the traveling-wave-like conductance configuration and the oscillating temperature T_b of two-terminal unbiased reservoirs $\mathbf{T}_b(t) = T_b(t)(1,1)^{\mathrm{T}}$, the saturated geometric pumped heat Q_{geo} is reached when the driving period τ_p becomes large enough, as shown in Fig. 2(a). Q_{geo} results from the nontrivial geometric curvature $F_{\mu\nu}$ in the area encircled by the arrowed contour, as shown in Fig. 2(b).

Geometric no-pumping restrictions. Following our geometric theory, we derive here its consequence on two sets of no-pumping theorems. First, fixing unbiased $\mathbf{T}_b$, we show $Q_{\text{geo}} = 0$ as long as the thermal conductance and capacity are not simultaneously driven. The vanishing of Q_{geo} is valid both for currents inside the system and that exchanged with reservoirs. This no-go restriction is not dependent on the number of reservoirs. In this class of protocols, the steady state $\mathbf{T}_{\text{ss}}$ remains intact in equilibrium with reservoirs during the whole process, resulting in zero geometric connection A_μ and curvature $F_{\mu\nu}$. Obviously no geometric pump effect is present here.

Second, we consider two-terminal systems with nonzero static thermal bias, which are generally focused on in recent discussions of diffusive nonreciprocity [24,55,56]. We prove that Q_{geo} between the system and reservoirs is always zero if either capacity or the conductance is driven. In the case of driving $\mathcal{C}$, $Q_{\text{geo}} = 0$ is easily shown by observing the independence of $\mathbf{T}_{\text{ss}}$ on $\mathcal{C}$. In contrast, $Q_{\text{geo}} = 0$ in the situation of driven conductance is a consequence of a symmetry in $F_{\mu\nu}$, i.e., $(F_{\mu\nu})^{\mathrm{T}} = -F_{\mu\nu}$. Since $F_{\mu\nu}$ as a number satisfies $(F_{\mu\nu})^{\mathrm{T}} = F_{\mu\nu}$, we obtain $F_{\mu\nu} = 0$ and $Q_{\text{geo}} = 0$ for this set of protocols so that the no-go restriction is present. For a detailed explanation, see Sec. III of the Supplemental Material [51].

Therefore, to introduce nontrivial $F_{\mu\nu}$, one should simultaneously modulate the conductance and reservoir temperature $\mathbf{T}_b$, or in addition modulate the capacity. As an illustration, we show in Fig. 3 the no-pumping restriction and its implication
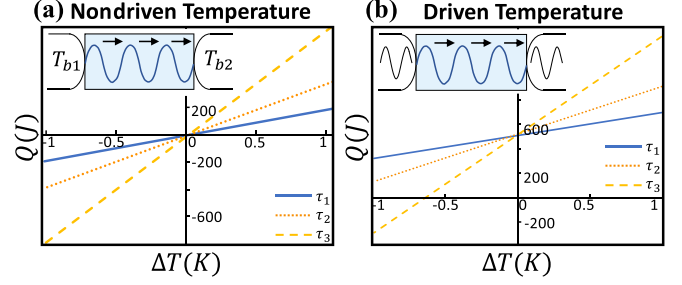

FIG. 3. The no-pumping condition and its implication on thermal nonreciprocity. (a) The no-pumping situation where the conductance is spatiotemporally driven while the reservoirs are fixed at $\mathbf{T}_b = (T_{b1}, T_{b2})$. The heat transferred during a driving period (τ_i, $i = 1, 2, 3$) is reciprocal with respect to the thermal bias $\Delta T \equiv T_{b1} - T_{b2}$. (b) The pumping and nonreciprocal situation. The conductance is driven in the form of a traveling wave and $\mathbf{T}_b$ is driven in phase. The protocol of the reservoir temperature is $\mathbf{T}_b(t) = [\sin(2\pi t/\tau_i)/2 + 1](T_{b1}, T_{b2})^{\mathrm{T}}$. Here, $T_{b1} = 30\,^\circ\mathrm{C}$. The driving periods are respectively $\tau_1 = 2.47 \times 10^4$ s, $\tau_2 = 7.02 \times 10^4$ s, and $\tau_3 = 2.00 \times 10^5$ s. Other parameters are the same as in Fig. 2.

on the nonreciprocity. The mere driving of conductance has no pumping effect and the transport is reciprocal [Fig. 3(a)]. In contrast, when reservoir temperatures are also driven, the emergent nontrivial Q_{geo} (Fig. 2) induces nonreciprocal transport, as demonstrated in Fig. 3(b). This elucidates that the nonzero Q_{geo} is a natural resource for generating thermal nonreciprocity, since Q_{geo} is not constrained by the temporal average thermal bias $\Delta T \equiv \langle T_{b1} \rangle - \langle T_{b2} \rangle$, but only reversed upon the retrorse driving protocol. We note this does not contradict the second law of thermodynamics. The total entropy production as sum of the dynamic and geometric parts is always non-negative.

A recent study involving both driven conductance and capacity demonstrates nonreciprocal diffusion [55]. Also, nonbroken thermal reciprocity has been observed in Ref. [56], since the thermal capacity is not allowed to be freely modulated. These concrete examples provide additional examples testifying to our geometric theory and no-pumping restrictions.

Trotterized switching driving protocol. A continuous and adiabatic driving protocol can be Trotterized into M pieces, with the system parameters being constant within each τ_p/M duration, as depicted in Figs. 1(c) and 1(d). Accordingly, the dynamic and geometric components of the accumulated heat are replaced by $Q_{\text{dyn}} = \sum_{m=1}^{M} (\mathbf{1} \cdot \mathcal{K}_c^m \mathbf{T}_{\text{ss}}^m + \mathbf{1} \cdot \mathcal{K}_b^m \mathbf{T}_b^m) \tau_p/M$, $Q_{\text{geo}} = \sum_{m=1}^{M} \mathbf{k}^m \cdot \Delta \mathbf{T}_{\text{ss}}^m$. Q_{geo} has a nature comparable with the Pancharatnam phase [57]. $\mathcal{K}_c^m$, $\mathcal{K}_b^m$, and $\mathbf{k}^m$ correspond to the system parameters in the mth ($1 \leqslant m \leqslant M$) protocol piece. The difference between the two adjacent steady states defines $\Delta \mathbf{T}_{\text{ss}}^m \equiv \mathbf{T}_{\text{ss}}^m - \mathbf{T}_{\text{ss}}^{m-1}$ (see Sec. IV in the Supplemental Material [51] for details).

Our experiment concerns a limit case, where parameters are cyclically switched between only two states, and the geometrically pumped heat is

$$Q_{\text{geo}} = (\mathbf{k}^1 - \mathbf{k}^2) \cdot (\mathbf{T}_{\text{ss}}^1 - \mathbf{T}_{\text{ss}}^2). \tag{6}$$

It is worth noting that the geometric effect of two-state switching is always zero in Hermitian quantum mechanics [58].

To produce a nonzero geometric effect, a driven Hermitian system at least requires a three-state cyclic switching to form a finite area in parameter space. Here, owing to the non-Hermiticity of nonequilibrium diffusive systems, the geometric effect for two-state switching exists once $(\mathbf{k}^m; \mathbf{T}^m_{ss})$ of two states are different from each other [shown in Fig. 1(d)]. This can be intuitively understood as the effect induced by the asymmetric rectified heat conduction in the time domain. Since $\mathbf{k}^m$ determines the accumulated current during the system's relaxation towards $\mathbf{T}^m_{ss}$, the nonvanishing Q_{geo} originates from the asymmetric response of the two different states $\mathbf{k}^1$ and $\mathbf{k}^2$ to an inverse nonequilibrium variation $\mathbf{T}^1_{ss} - \mathbf{T}^2_{ss}$. This behaves as a temporal thermal diode and rectifier.

Experimental demonstration. Under the guidance of geometric no-pumping theorems, we devise a minimal experiment setup to observe nonzero Q_{geo}, with both heat conductances and reservoir temperatures being modulated, as shown in Fig. 4(a). We connect both ends of the copper plate to the thermal reservoirs with instantaneously identical temperatures T_b. The thermal conductance between the copper plate and two reservoirs, i.e., κ_1 and κ_2, are out of phase. The protocol is shown in Fig. 4(b) (see Sec. V of the Supplemental Material [51] for details). We calibrate the effective conductances κ_n with the maximum $\kappa = 0.049$ W/K to account for the presence of dissipation in the surrounding atmosphere. We also calibrate the maximum and minimum temperature of the effective thermal reservoir T_b as $T_{hot} = 35.2\,°C$ and $T_{cold} = 14.8\,°C$. Figure 4(c) is an infrared imaging snapshot of Fig. 4(a). To conveniently modulate κ_1 and κ_2 in the experiment, we construct the system-reservoir couplings with two types of reversible shape memory alloys (SMAs). The geometric configurations of SMA change rapidly as its temperature varies, which is also applied in devising macroscopic thermal diodes [59].

The measured result of pumped Q is shown in Fig. 4(d) as dots. It is theoretically described by $Q = \Delta T_b C \tanh[\kappa \tau_p/(4C)]$ shown as the black line, where C is the heat capacity of the central system, $\Delta T_b \equiv T_{hot} - T_{cold}$. In our experimental setup, $C = 26.208$ J/K and $\Delta T_b = 20.4\,°C$. The dynamical heat component is $Q_{dyn} \equiv 0$ due to the strict instantaneous zero bias of the thermal reservoirs. The pumped heat is singly attributed to the geometric contribution Q_{geo}. To verify our general theory on driven thermal diffusion, we concentrate on the limits ($\tau_p \ll \tau_c \equiv 4C/\kappa$ and $\tau_p \gg \tau_c$). After the system enters a cyclic state, we measure the heat transferred during each period under different driving periods τ_p. In the fast driving region, Q and τ_p are approximately linearly correlated, consistent with $Q \approx \kappa \Delta T_b \tau_p/4$. In the adiabatic limit ($\tau_p \gg \tau_c$), Q remains unchanged as τ_p varies, and its experimental plateau value is $Q_{geo} = 546$ J. To verify our general geometric theory, we note that steady states $\mathbf{T}^n_{ss} = T^n_b$ ($n = $ I, II labeling different configurations). Also, defining the positive direction of the current as left to right, $\mathcal{M}^n_c = -(\kappa^n_1 + \kappa^n_2)/C$ and $\mathcal{K}^n_b = (-\kappa^n_1, \kappa^n_2)^T/C$. Without losing generality, we select $\mathbf{1} = (1, 0)^T$. Thus, $\mathbf{k}^1 - \mathbf{k}^2 = C$ and Eq. (6) reduces to $Q_{geo} = C\Delta T_b$, in agreement with our measurement result, showing Q in our experiment to be purely geometric. This proves the existence of general geometric heat pump effects in the classical diffusive transport.
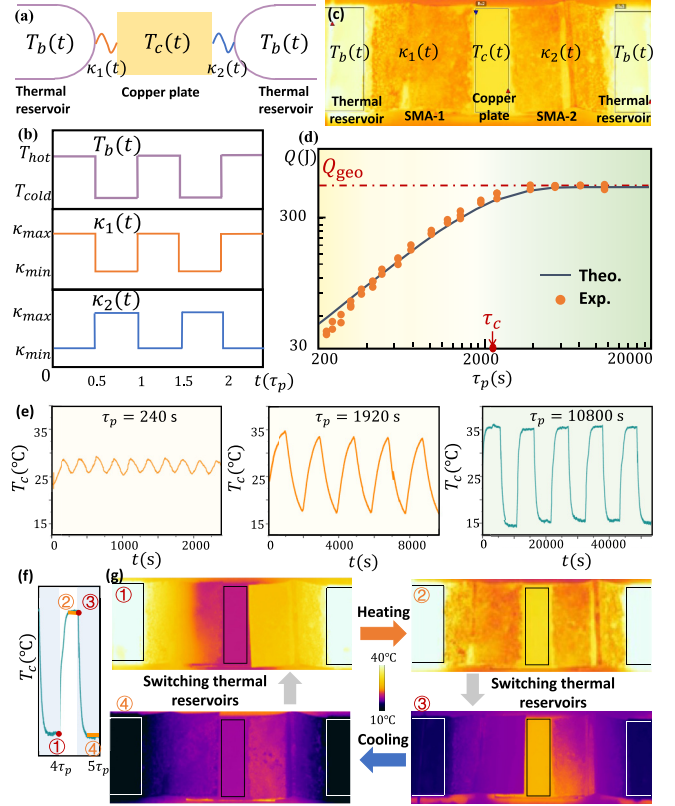

FIG. 4. Observation of a geometric heat pump in a thermal diffusion system. (a) The schematic diagram of the experimental setup, where the identical temperature of two reservoirs T_b and the thermal conductances κ_n ($n = 1, 2$) are driven periodically by (b). (c) A snapshot of the experimental device generated by an infrared thermal imager, corresponding to (a). (d) The heat transferred during a single driving period vs different τ_p. The characteristic time $\tau_c \equiv 4C/\kappa = 2140$ s signifies fast driving and slow driving, marked by the yellow and green background color, respectively. The geometric heat pump effect is observed as the plateau $Q_{geo} = 546$ J. (e) The evolution of T_c in different τ_p situations, corresponding to the fast and slow driving cases in (d). The maximum and minimum of T_c get closer to that of the thermal reservoirs as τ_p gets longer. (f) A typical period in the evolution of T_c ($\tau_p = 10\,800$ s), which contains four phases. The background colors distinguish the different parameter states. (g) Snapshots of the four phases in (f) in the adiabatic limit.

To further analyze the pump process, Fig. 4(e) shows the variations of the copper plate's temperature T_c in different driving periods τ_p, representing the two cases—the fast driving (yellow background) and slow driving (green background). In the adiabatic limit (e.g., $\tau_p = 10\,800$ s), the thermodynamic process consists of four phases in one period, which are marked as ①, ②, ③, ④ in Fig. 4(f). We display the details of the four phases with infrared imaging snapshots in Fig. 4(g). From phase ① to ② and phase ③ to ④, the middle T_c shuttles heat between two reservoirs. This shuttled heat is evidently independent of the driving period in the slow driving limit. Our devised simple setup attributes the geometrically pumped heat, expressed by Eqs. (5) and (6), to the changing of system states and the intrinsic geometric properties of the parameter space.

Conclusion. By formulating a geometric theory on driven thermal diffusion, we demonstrate straightforward ways of determining no-pumping restrictions and construct thermal nonreciprocity based on protocol designs. The nonvanishing geometric heat flow works as a versatile and reliable resource in generating directional heat flow, harnessing thermal energy, and generating thermal nonreciprocity by devising a dynamical toolkit. Constructing geometric effect-induced topologically protected phenomena in driven thermal radiation [60] constitutes a promising task.

Although we focus here on thermal diffusion described by Fourier's law, our theory can be readily adapted to general macroscopic diffusion. For example, by replacing the thermal conductance (temperature, heat capacity) with mass conductance (chemical potential, mass capacity) [55,61],

the geometric pump effect and no-pumping restrictions can be readily transplanted to the driven mass diffusion governed by Fick's law (shown in Fig. S1 of the Supplemental Material [51]). The extension of geometric pumping and no-go restriction to macroscopic systems involving coupled diffusive dynamics, e.g., thermoelectric transport, coupled heat-mass-charge transfer, complex convection-conduction transport, etc., is also a promising topic for the future.

[1] A. Dhar, Adv. Phys. **57**, 457 (2008).
[2] N. Li, J. Ren, L. Wang, G. Zhang, P. Hänggi, and B. Li, Rev. Mod. Phys. **84**, 1045 (2012).
[3] S. Yang, J. Wang, G. Dai, F. Yang, and J. Huang, Phys. Rep. **908**, 1 (2021).
[4] Y. Li, W. Li, T. Han, X. Zheng, J. Li, B. Li, S. Fan, and C.-W. Qiu, Nat. Rev. Mater. **6**, 488 (2021).
[5] K. Saito and A. Dhar, Phys. Rev. Lett. **99**, 180601 (2007).
[6] S. Saryal, H. M. Friedman, D. Segal, and B. K. Agarwalla, Phys. Rev. E **100**, 042101 (2019).
[7] P. Talkner and P. Hänggi, Rev. Mod. Phys. **92**, 041002 (2020).
[8] B. Li, L. Wang, and G. Casati, Phys. Rev. Lett. **93**, 184301 (2004).
[9] C. W. Chang, D. Okawa, A. Majumdar, and A. Zettl, Science **314**, 1121 (2006).
[10] P. Ben-Abdallah and S.-A. Biehs, Phys. Rev. Lett. **112**, 044301 (2014).
[11] K. Joulain, J. Drevillon, Y. Ezzahri, and J. Ordonez-Miranda, Phys. Rev. Lett. **116**, 200601 (2016).
[12] S. Narayana and Y. Sato, Phys. Rev. Lett. **108**, 214303 (2012).
[13] R. Schittny, M. Kadic, S. Guenneau, and M. Wegener, Phys. Rev. Lett. **110**, 195901 (2013).
[14] H. Xu, X. Shi, F. Gao, H. Sun, and B. Zhang, Phys. Rev. Lett. **112**, 054301 (2014).
[15] T. Han, X. Bai, D. Gao, J. T. L. Thong, B. Li, and C.-W. Qiu, Phys. Rev. Lett. **112**, 054302 (2014).
[16] Y. Ma, Y. Liu, M. Raza, Y. Wang, and S. He, Phys. Rev. Lett. **113**, 205501 (2014).
[17] T. Kitagawa, E. Berg, M. Rudner, and E. Demler, Phys. Rev. B **82**, 235114 (2010).
[18] W. Ma, L. Zhou, Q. Zhang, M. Li, C. Cheng, J. Geng, X. Rong, F. Shi, J. Gong, and J. Du, Phys. Rev. Lett. **120**, 120501 (2018).
[19] G. Engelhardt, G. Platero, and J. Cao, Phys. Rev. Lett. **123**, 120602 (2019).
[20] G. Engelhardt and J. Cao, Phys. Rev. Lett. **126**, 090601 (2021).
[21] N. Li, P. Hänggi, and B. Li, Europhys. Lett. **84**, 40009 (2008).
[22] J. Ren and B. Li, Phys. Rev. E **81**, 021111 (2010).
[23] R. Marathe, A. M. Jayannavar, and A. Dhar, Phys. Rev. E **75**, 030103(R) (2007).
[24] D. Torrent, O. Poncelet, and J.-C. Batsale, Phys. Rev. Lett. **120**, 125501 (2018).

[25] S. Buddhiraju, W. Li, and S. Fan, Phys. Rev. Lett. **124**, 077402 (2020).
[26] I. Latella, R. Messina, J. M. Rubi, and P. Ben-Abdallah, Phys. Rev. Lett. **121**, 023903 (2018).
[27] H. Li, L. J. Fernández-Alcázar, F. Ellis, B. Shapiro, and T. Kottos, Phys. Rev. Lett. **123**, 165901 (2019).
[28] Y. Wang, Z. Zhang, T. Usui, M. Benedict, S. Hirose, J. Lee, J. Kalb, and D. Schwartz, Science **370**, 129 (2020).
[29] Y. Li, Y.-G. Peng, L. Han, M.-A. Miri, W. Li, M. Xiao, X.-F. Zhu, J. Zhao, A. Alù, S. Fan *et al.*, Science **364**, 170 (2019).
[30] G. Xu, Y. Li, W. Li, S. Fan, and C.-W. Qiu, Phys. Rev. Lett. **127**, 105901 (2021).
[31] M. V. Berry, Proc. R. Soc. A **392**, 45 (1984).
[32] D. J. Thouless, Phys. Rev. B **27**, 6083 (1983).
[33] P. W. Brouwer, Phys. Rev. B **58**, R10135 (1998).
[34] N. A. Sinitsyn and I. Nemenman, Phys. Rev. Lett. **99**, 220408 (2007).
[35] R. D. Astumian and P. Hänggi, Phys. Today **55** (11), 33 (2002).
[36] V. Y. Chernyak and N. A. Sinitsyn, Phys. Rev. Lett. **101**, 160601 (2008).
[37] S. Rahav, J. Horowitz, and C. Jarzynski, Phys. Rev. Lett. **101**, 140602 (2008).
[38] J. Ren, P. Hänggi, and B. Li, Phys. Rev. Lett. **104**, 170601 (2010).
[39] T. Chen, X.-B. Wang, and J. Ren, Phys. Rev. B **87**, 144303 (2013).
[40] C. Wang, J. Ren, and J. Cao, Phys. Rev. A **95**, 023610 (2017).
[41] W. Nie, G. Li, X. Li, A. Chen, Y. Lan, and S.-Y. Zhu, Phys. Rev. A **102**, 043512 (2020).
[42] J. Ren, S. Liu, and B. Li, Phys. Rev. Lett. **108**, 210603 (2012).
[43] T. Sagawa and H. Hayakawa, Phys. Rev. E **84**, 051110 (2011).
[44] K. Brandner and K. Saito, Phys. Rev. Lett. **124**, 040602 (2020).
[45] B. Bhandari, P. T. Alonso, F. Taddei, F. von Oppen, R. Fazio, and L. Arrachea, Phys. Rev. B **102**, 155407 (2020).
[46] Y. Hino and H. Hayakawa, Phys. Rev. Research **3**, 013187 (2021).
[47] K. Funo, N. Lambert, F. Nori, and C. Flindt, Phys. Rev. Lett. **124**, 150603 (2020).
[48] K. Takahashi, K. Fujii, Y. Hino, and H. Hayakawa, Phys. Rev. Lett. **124**, 150602 (2020).

[49] Z. Wang, L. Wang, J. Chen, C. Wang, and J. Ren, Front. Phys. **17**, 13201 (2022).

[50] H. B. Callen, *Thermodynamics and an Introduction to Thermostatistics* (Wiley, New York, 1985).

[51] See Supplemental Material at http://link.aps.org/supplemental/10.1103/PhysRevE.106.L032102 for details, which includes Refs. [24,52–54,61].

[52] Y. Aharonov and J. Anandan, Phys. Rev. Lett. **58**, 1593 (1987).

[53] M. Bukov, L. D'Alessio, and A. Polkovnikov, Adv. Phys. **64**, 139 (2015).

[54] M. Kolodrubetz, D. Sels, P. Mehta, and A. Polkovnikov, Phys. Rep. **697**, 1 (2017).

[55] M. Camacho, B. Edwards, and N. Engheta, Nat. Commun. **11**, 3733 (2020).

[56] J. Li, Y. Li, P.-C. Cao, X. Zheng, Y.-G. Peng, B. Li, X.-F. Zhu, A. Alù, and C.-W. Qiu, Nat. Commun. **13**, 167 (2022).

[57] S. Pancharatnam, Proc. Indian Acad. Sci. A **44**, 398 (1956).

[58] R. Resta, Eur. Phys. J. B **79**, 121 (2011).

[59] Y. Li, X. Shen, Z. Wu, J. Huang, Y. Chen, Y. Ni, and J. Huang, Phys. Rev. Lett. **115**, 195503 (2015).

[60] L. J. Fernández-Alcázar, R. Kononchuk, H. Li, and T. Kottos, Phys. Rev. Lett. **126**, 204101 (2021).

[61] B. Gebhart, *Heat Conduction and Mass Diffusion*, Vol. 634 (McGraw-Hill, New York, 1993).